FERMILAB-CONF-76-125-E

Presented to Tblisi conf. July 1976

Title:- Measurements of the Nucleon Structure Function in Muon Deep Inelastic Scattering at 100 and 150 GeV/c.

H.L. Anderson, V.K. Bharadwaj, N.E. Booth, R.M. Fine, W.R. Francis, B.A. Gordon, R.H. Heisterberg, R.G. Hicks, T.B.W. Kirk, G.I. Kirkbride, W.A. Loomis, H.S. Matis, L.W. Mo, L.C. Myrianthopoulos, F.M. Pipkin, S.H. Pordes, T.W. Quirk, W.D. Shambroom, A. Skuja, L.J. Verhey, W.S.C. Williams, Richard Wilson and S.C. Wright

Enrico Fermi Institute and Department of Physics, The University of Chicago, Chicago, Illinois 60637, and High Energy Physics Laboratory and Department of Physics, Harvard University, Cambridge, Massachusetts, 02138, and Department of Physics, The University of Illinois at Urbana-Champaign, Urbana, Illinois 61801, and Department of Nuclear Physics, The University of Oxford, Oxford OX1 3RH, England

Abstract:- This paper presents the results of the analysis of a deep inelastic scattering experiment using 100 and 150 GeV muons incident on a liquid hydrogen target.

Values of the proton structure function νW_2 are presented in the region $0.2 < q^2 < 50$ $(GeV/c)^2$ and $5 < \nu < 130$ GeV. A limit is set on $R = \sigma_L/\sigma_T$ in a restricted kinematic region.

The data is combined with previous deuterium measurements to provide a neutron-proton comparison and to evaluate sum rules.

We report the results of a preliminary analysis of inelastic scattering of 100 and 150 GeV muons from a liquid hydrogen target.

We limit this report to presenting the interesting features of the data rather than a comprehensive presentation over the entire kinematic region covered by the experiment.

The differential cross-section for the scattering of muons of energy E to a final energy E' through an angle θ is related to the two inelastic structure functions W_1 and W_2 by[1]

$$\frac{d^2\sigma}{d\nu dq^2} = \frac{\pi}{pp'} \frac{2\alpha^2}{q^4} \left(\frac{p'}{p}\right) \left[(2EE' - q^2/2)\ W_2\ (q^2,\nu) + (q^2 - 2M_\mu^{\ 2})\ W_1(q^2,\nu)\right]$$

where $\nu = E - E'$ and $q^2 = 2(EE' - pp' \cos\theta - M\mu^2)$

The ratio of the inelastic structure functions can be expressed as $W_1/W_2 = (1 + \nu^2/q^2)/(1 + R)$ where $R = \sigma_L/\sigma_T$, the ratio of the photo-absorption cross-sections for longitudinal and transverse photons. The differential cross-section may be written explicitly in terms of the virtual photo-absorption cross-sections[2]:

$$\frac{d^2\sigma}{d\nu dq^2} = \Gamma(E,\ E',\ \theta)\ [\sigma_T(\nu,q^2) + (\varepsilon + \delta)\ \sigma_L(\nu,q^2)]$$

where Γ is the virtual photon flux factor, $\delta = 2M_\mu^{\ 2}(1-\varepsilon)/q^2$

and $\varepsilon = 1/[1 + \frac{2(q^2 + \nu^2)\ \tan^2\theta/2}{q^2(1-q^2min/q^2)^2}$ is the ratio of the fluxes of longitudinal and transverse photons. The apparatus and its acceptance, the analysis method and radiative correction procedure have been briefly described elsewhere[3]. We present here data from 1.7×10^{10} incident muons at 100 GeV and 1.6×10^{10} incident muons at 150 GeV.

Figure 1 shows the proton structure function $F_2 = \nu W_2\ (\omega,q^2)$ as a function of q^2 for various values of ω ($\omega = 2m\nu/q^2$) using only the 150 GeV data and assuming R = 0.18. The data exhibits the features disclosed by previous measurements with νW_2 falling at low omega and rising at large omega with increasing q^2 [4,5,3]. It should be noted that our data in contrast with the SLAC data is not appreciably affected if it is rebinned using ω' or the Georgi-Politzer variable[6] where $1/\xi = \frac{\omega}{2}\left(1 + \sqrt{1 + \frac{4m_p^2}{q^2\omega^2}}\right)$

Figure 2 shows the same data plotted as a function of X (= $^1/\omega$) for various values of q^2. The data is shown combined with the precise low energy electra scattering measurements from SLAC[5]. The smooth curves are the results of fits to the data using the form $F_2(x) = \sum_{i=3}^{5} a_i(1-x)^i$. Figure 3 shows the resultant fits for all data sets. If the fits are used to extrapolate into regions not covered by the data points then $\int_0^1 F_2(x)dx = 0.18 \pm 0.01$[7] for each q^2 region.

Figure 4 shows the total photo-absorption cross-section $\sigma_T + \epsilon\sigma_L$ measured at 100 and 150 GeV in the region of q^2 from 1 to 6 $(GeV/c)^2$ and $W^2 (=2m\nu - q^2 + M_p^2)$ from 100 to 144 GeV^2. We find for q^2 from 1 to 2 $(GeV/c)^2$ R = -0.10 ± 0.27 and for q^2 from 2 to 6 $(GeV/c)^2$ R = 0.02 ± 0.30. The errors quoted are statistical and no allowance has been made for systematic errors. These results are compatible with the lower energy measurements of R[5] and indicate no substantial rise of R with increasing ω. An attractive and complete explanation of the behaviour of this data is to be found in renormalizable field theories[8]. The observed behaviour of $F_2(x)$ as a function of q^2, the constancy of the integral $\int_0^1 F_2(x)dx$ as a function of q^2 are predicted by these theories.

We sincerely thank the Fermilab and the support staff at Chicago, Harvard, Illinois, Oxford and the Rutherford Laboratory for their invaluable contribution to this experiment.

REFERENCES

1. S.D. Drell and J.D. Walecka, Ann. Phys. 28 18 (1964).

2. L.N. Hand, Phy. Rev. 129 1834 (1963).

3. W.A. Loomis et al, Phy. Rev. Letters 35, 1483 (1975)
   H.L. Anderson et al, Phy. Rev. Letters 36, 1422 (1976)
   H.L. Anderson et al, Phy. Rev. Letters, 37, 4(1976).

4. Y. Watanabe et al, Phy. Rev. Letters 35, 898 (1975).
   C. Chang et al, Phy. Rev. Letters 35, 901 (1975).

5. E.M. Riordan et al, Report No. SLAC-PUB-1634, SLAC, Stanford, California (1975).

6. H. Georgi and H.D. Politzer, Phy. Rev. Letters 36, 1281 (1976).

7. The absence of high x points for the data in the region q^2 from 1 to 2 $(GeV/c)^2$ leads to a larger error in $\int_0^1 F_2(x)dx$.

8. See H.D.Politzer, Phys. Reports 14C No. 4 (1974)
   K. Kogut and L. Susshind, Phy. Rev. D9, 697 (1974), and 3391 (1974).

Figure 1a to f

$\nu W_2^{\,P}$ as a function of q^2 for various ω bins. The triangles indicate data measured at SLAC by Riordan et al.[5]

Figure 2a to d

$F_2(x) = \nu W_2^{\,P}$ as a function of X for various q^2 bins. The triangles indicate data measured at SLAC by Riordan et al.[5] The solid curves are fits to the combined data.

Figure 3

$F_2(x)$ as a function of X showing the fitted curves for the data. The area under the curves remains constant.

Figure 4

$\sigma_T + \varepsilon\sigma_L$ as a function of ε, for various q^2 bins in the region $W^2 = 100 - 144$ GeV.

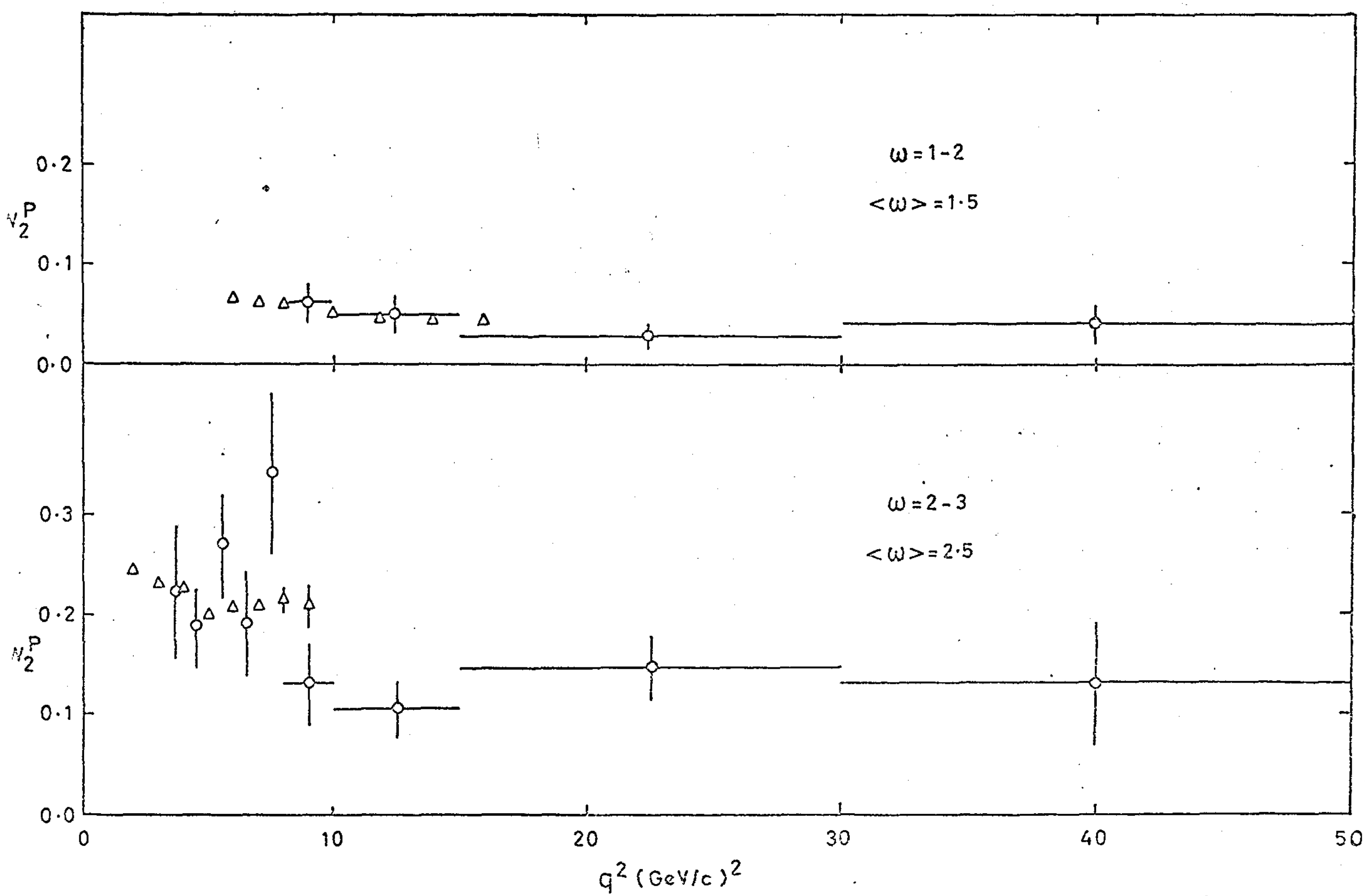

ω = 1-2
<ω> = 1·5
ω = 2-3
<ω> = 2·5
0·2
0·1
0·0
0·3
0·2
0·1
0·0
νW_2^P
νW_2^P
0
10
20
30
40
50
q² (GeV/c)²

Figure 1 a

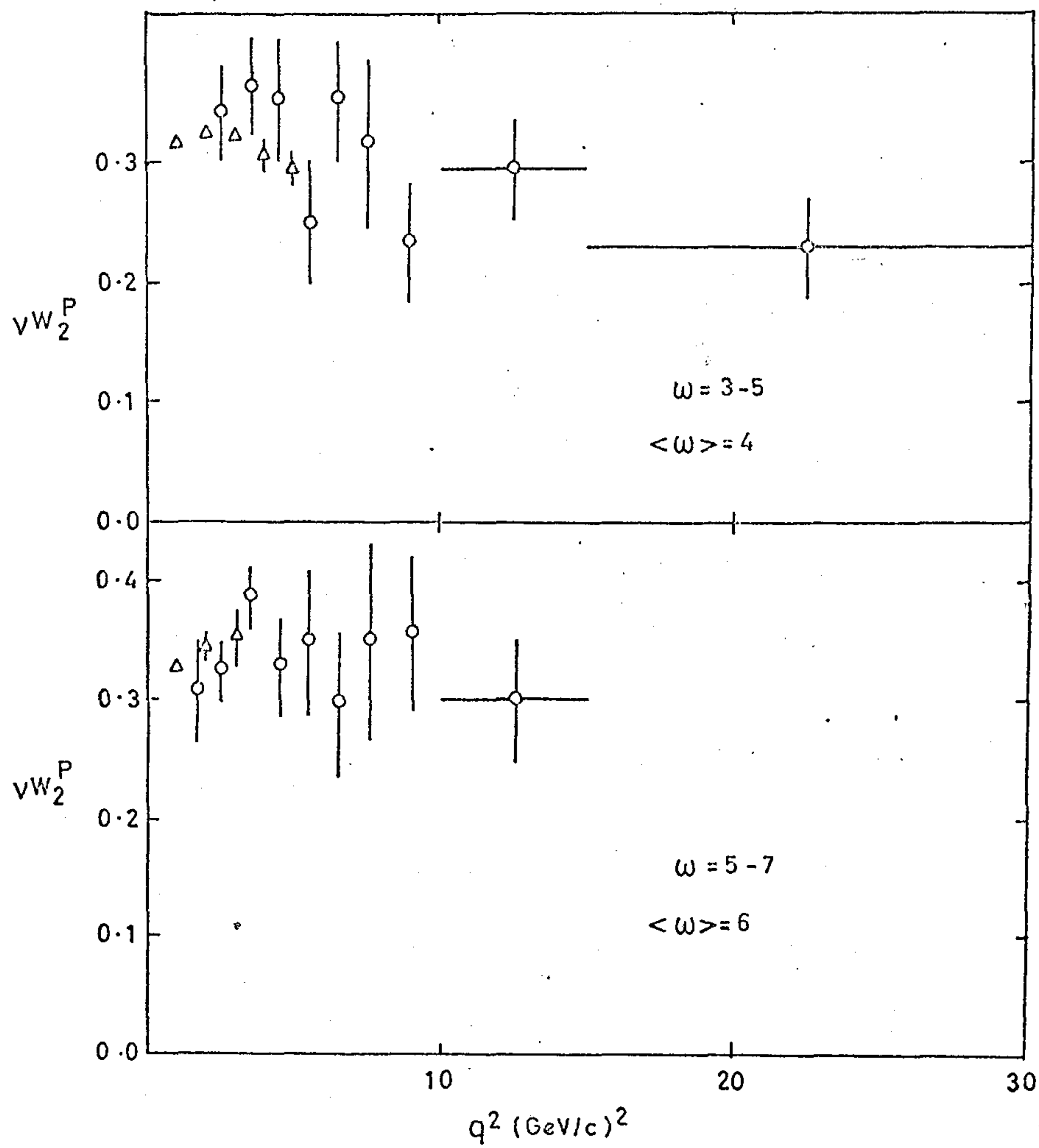
0·3
0·2
νW_2^P
0·1
ω = 3-5
<ω>= 4
0·0
0·4
0·3
νW_2^P
0·2
ω = 5 - 7
<ω>= 6
0·1
0·0
10
20
30
q^2 (GeV/c)^2

Figure 1 b

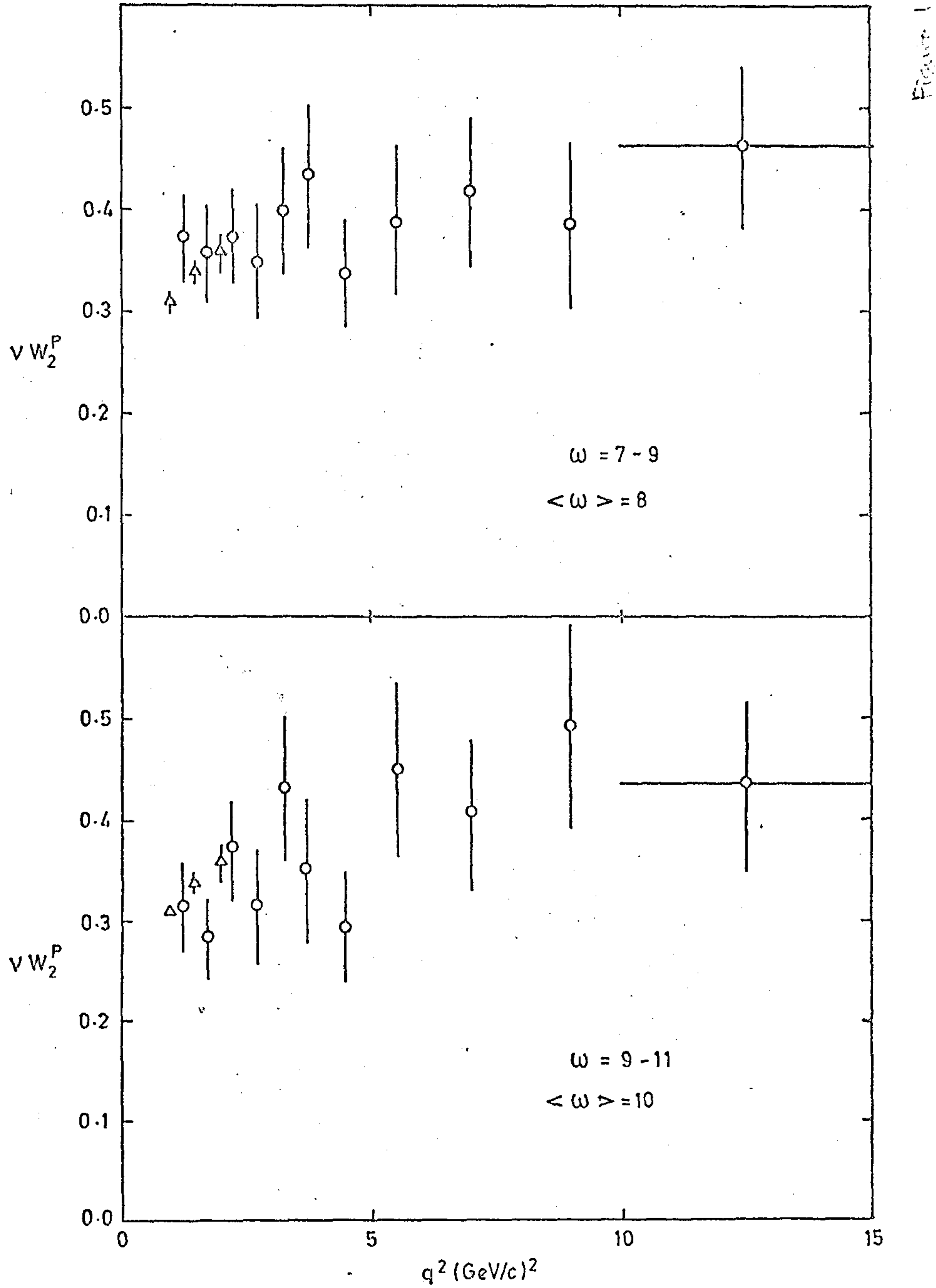
Figure 1
0·5
0·4
0·3
0·2
0·1
0·0
νW_2^P
ω = 7 - 9
< ω > = 8
ω = 9 - 11
< ω > = 10
0
5
10
15
q^2 (GeV/c)^2

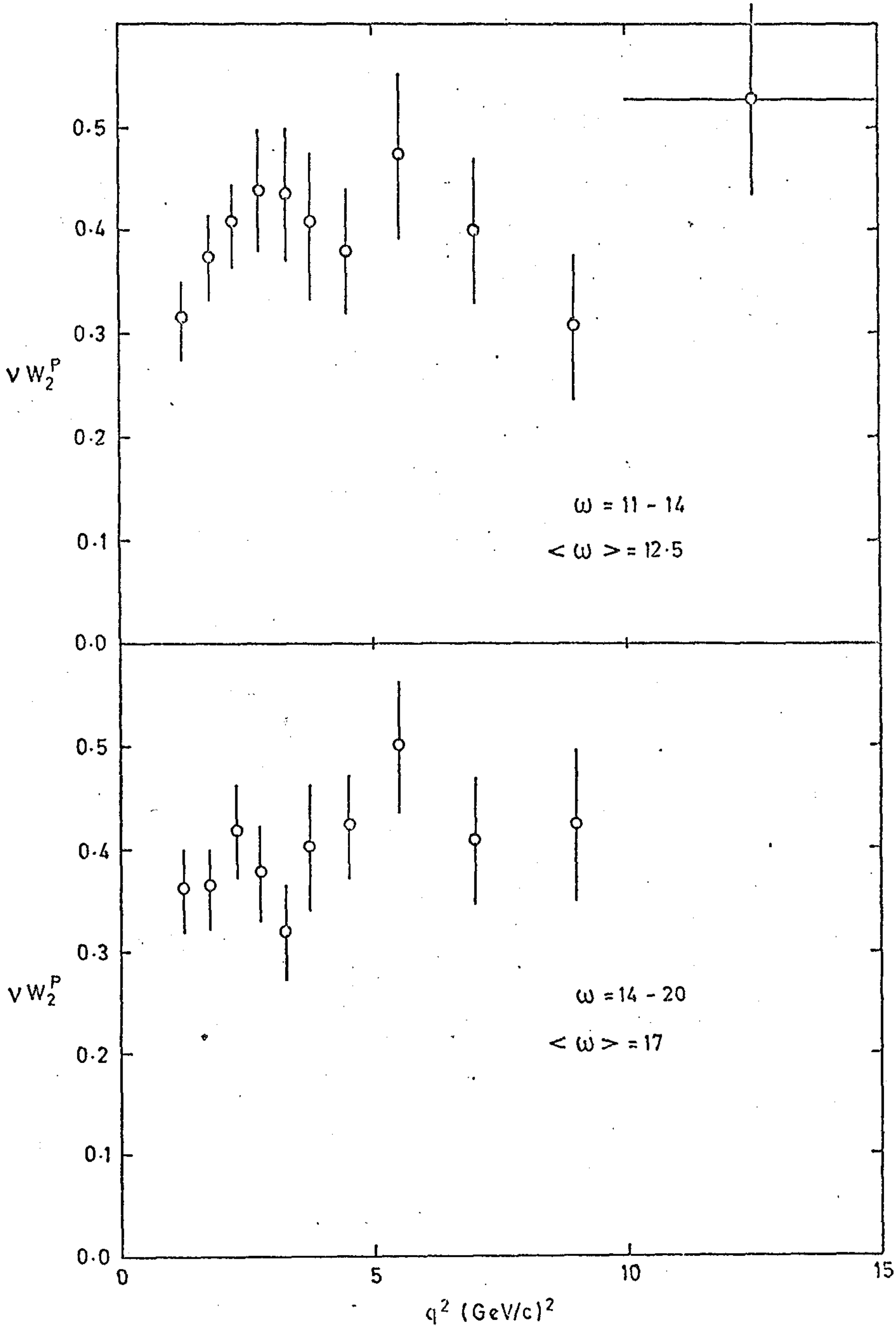

νW_2^P
ω = 11 - 14
< ω > = 12·5
νW_2^P
ω = 14 - 20
< ω > = 17
q^2 (GeV/c)^2

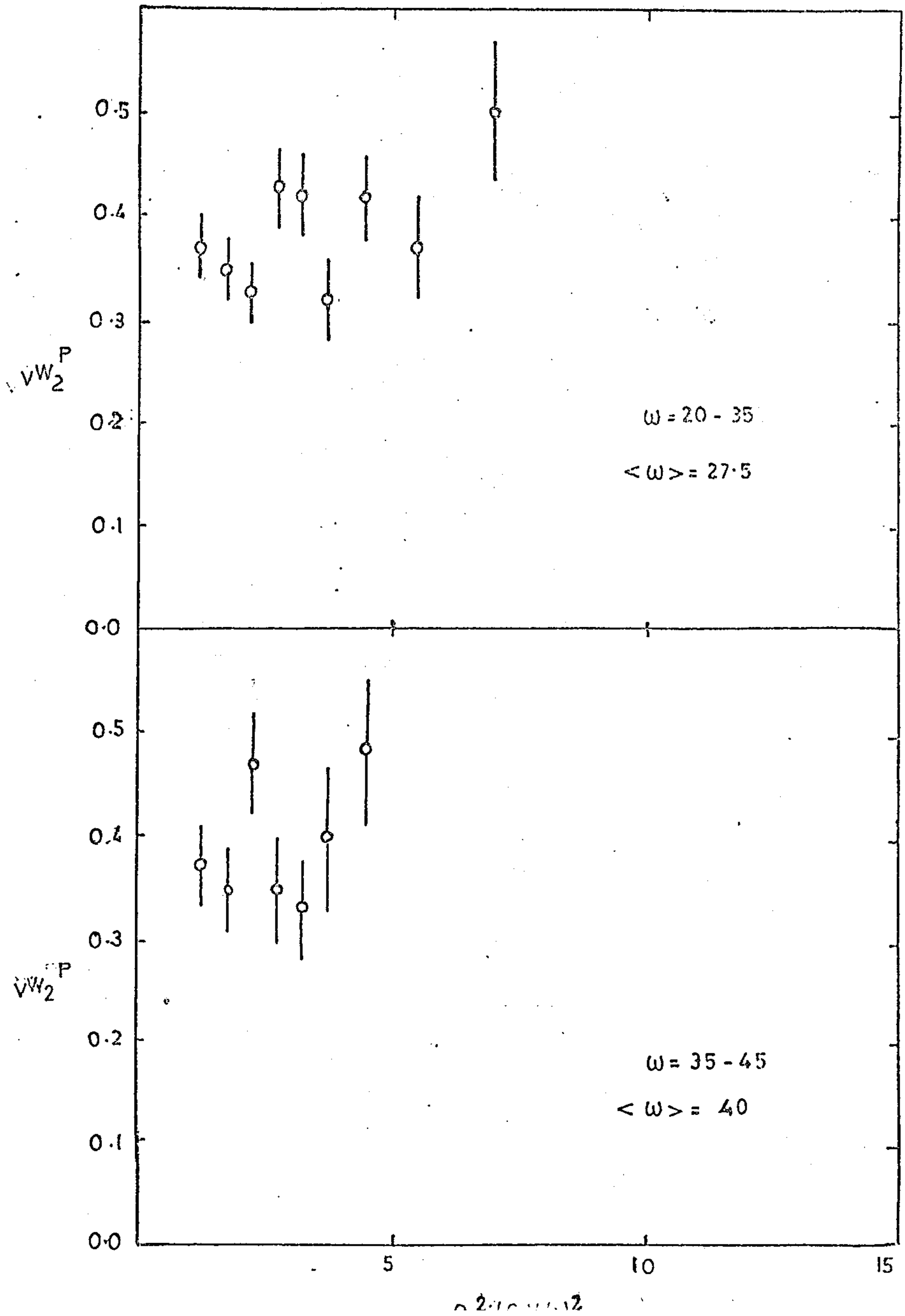

0·5
0·4
0·3
νW2P
0·2
0·1
0·0
ω = 20 - 35
< ω > = 27·5
0·5
0·4
0·3
νW2P
0·2
0·1
0·0
ω = 35 - 45
< ω > = 40
5
10
15

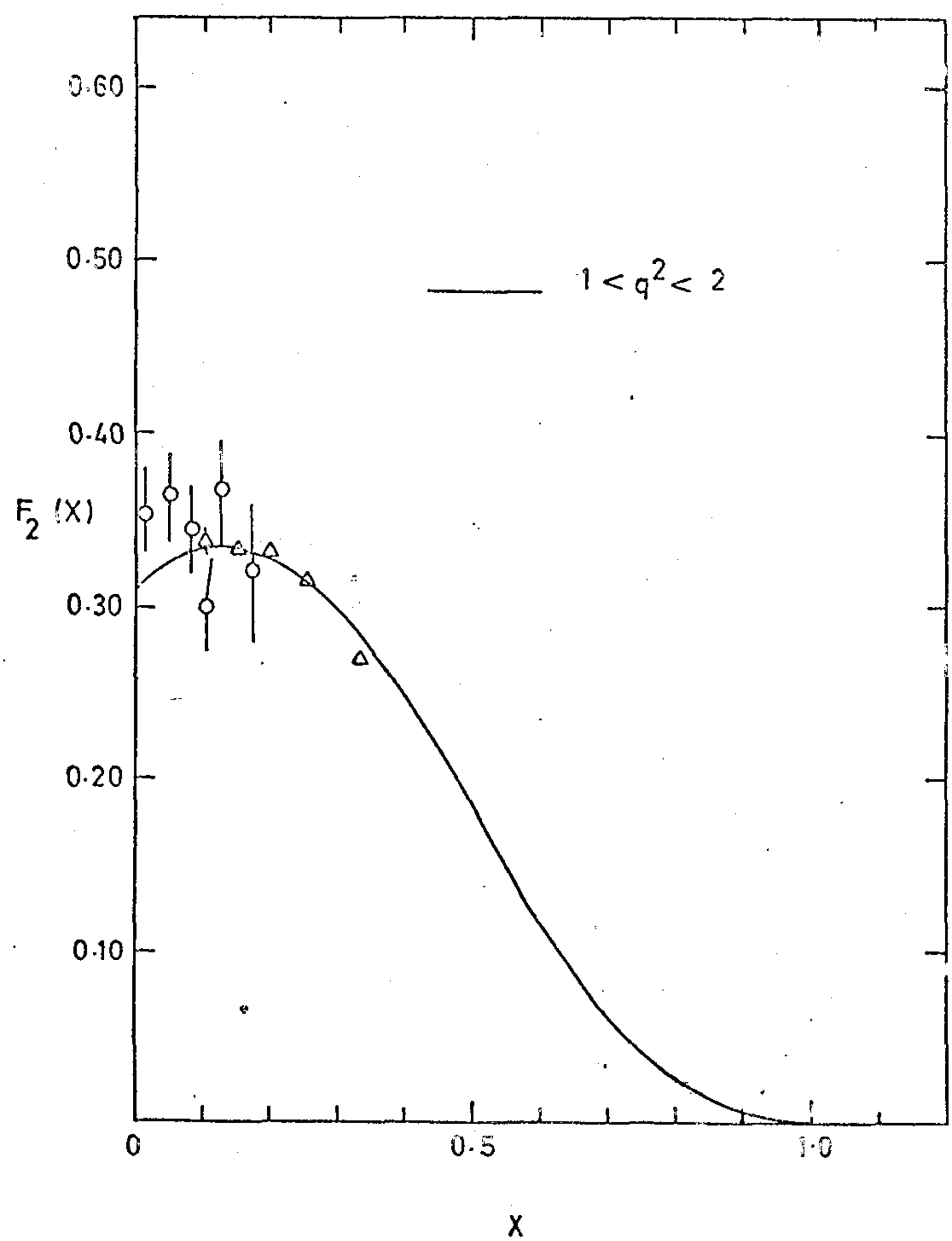
0·60
0·50
0·40
0·30
0·20
0·10
F_2 (X)
$1 < q^2 < 2$
0
0·5
1·0
X

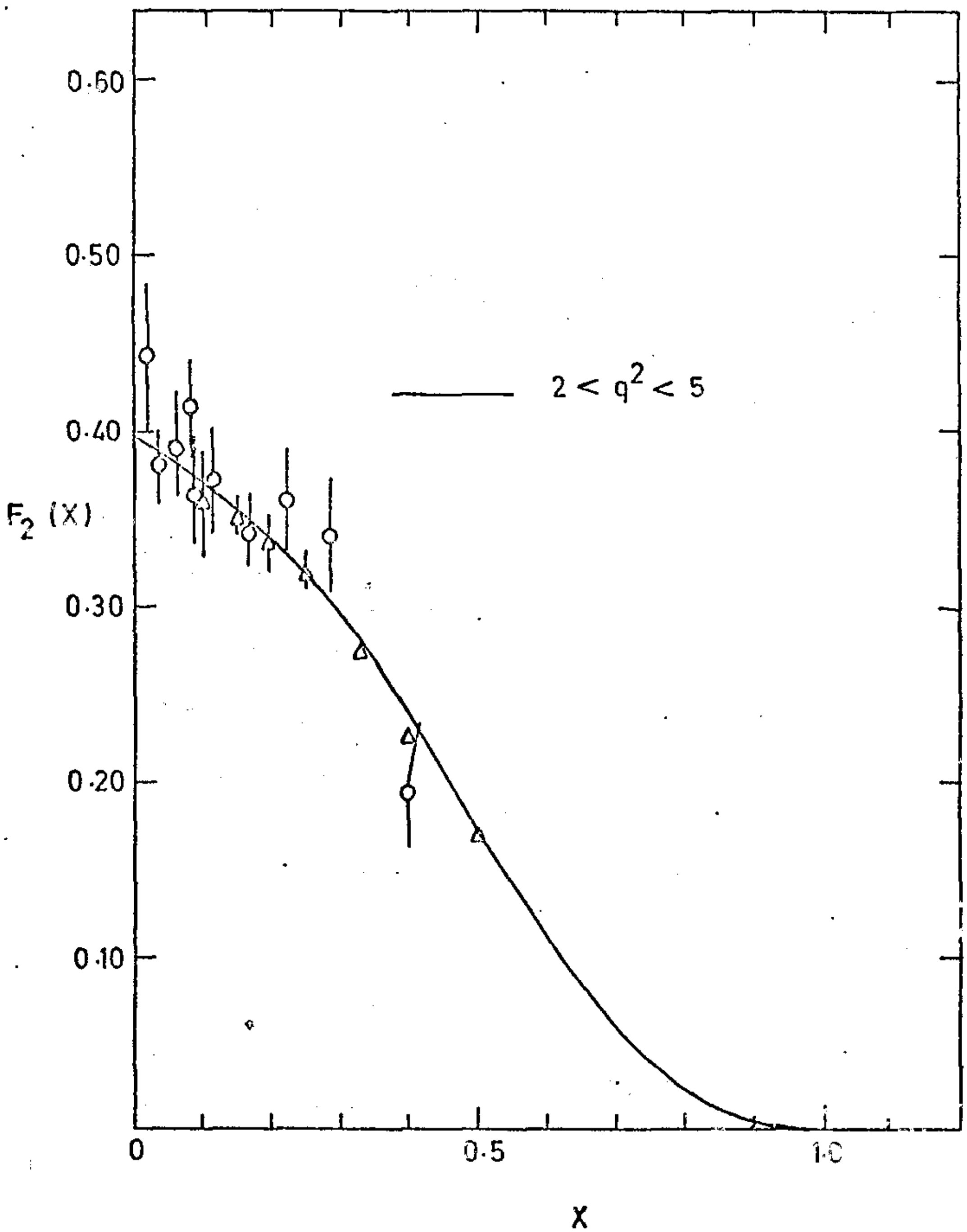
0·60
0·50
0·40
0·30
0·20
0·10
F_2 (X)
$2 < q^2 < 5$
0
0·5
1·0
X

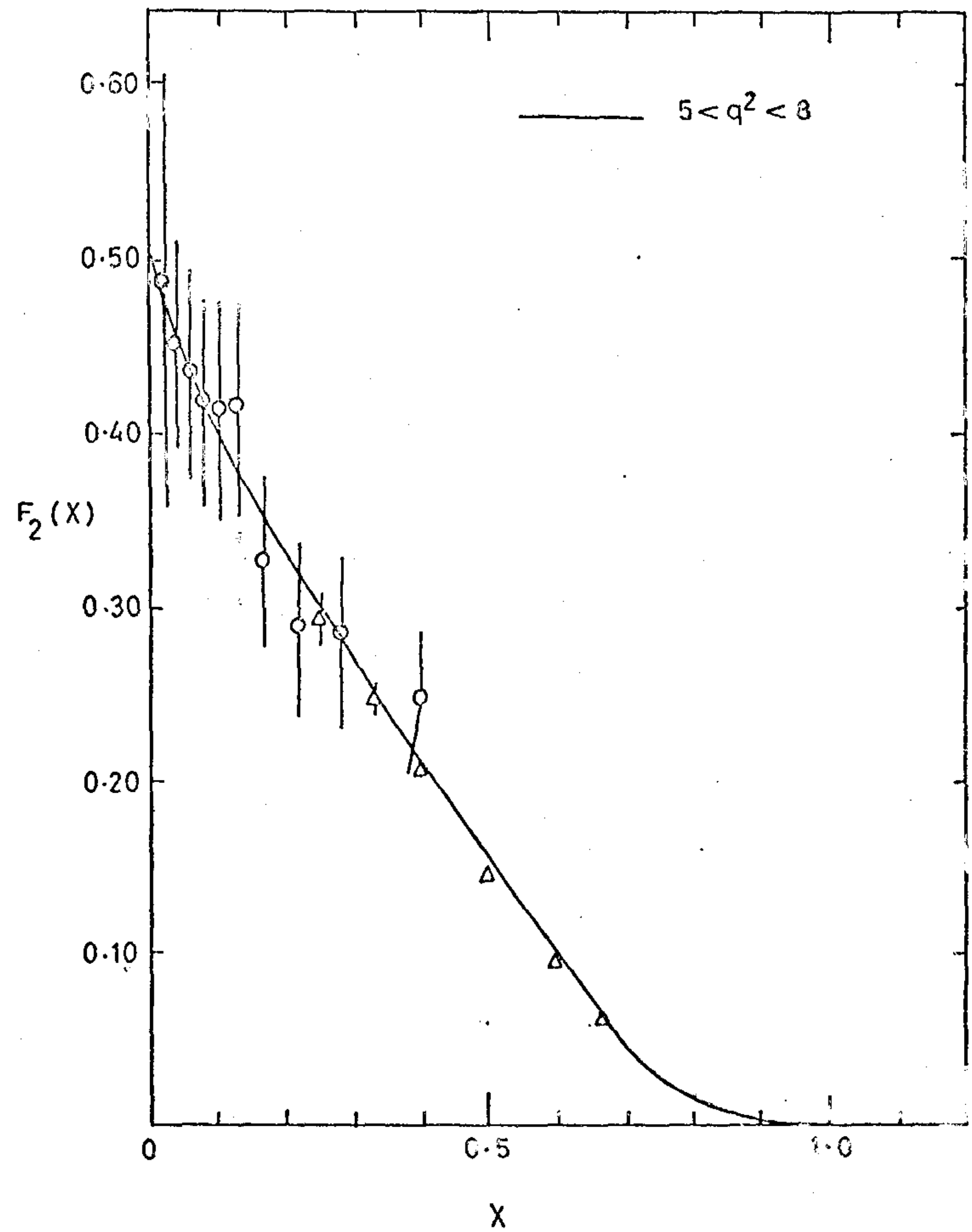

0·60
0·50
0·40
0·30
0·20
0·10
$F_2(X)$
$5 < q^2 < 8$
0
0·5
1·0
X

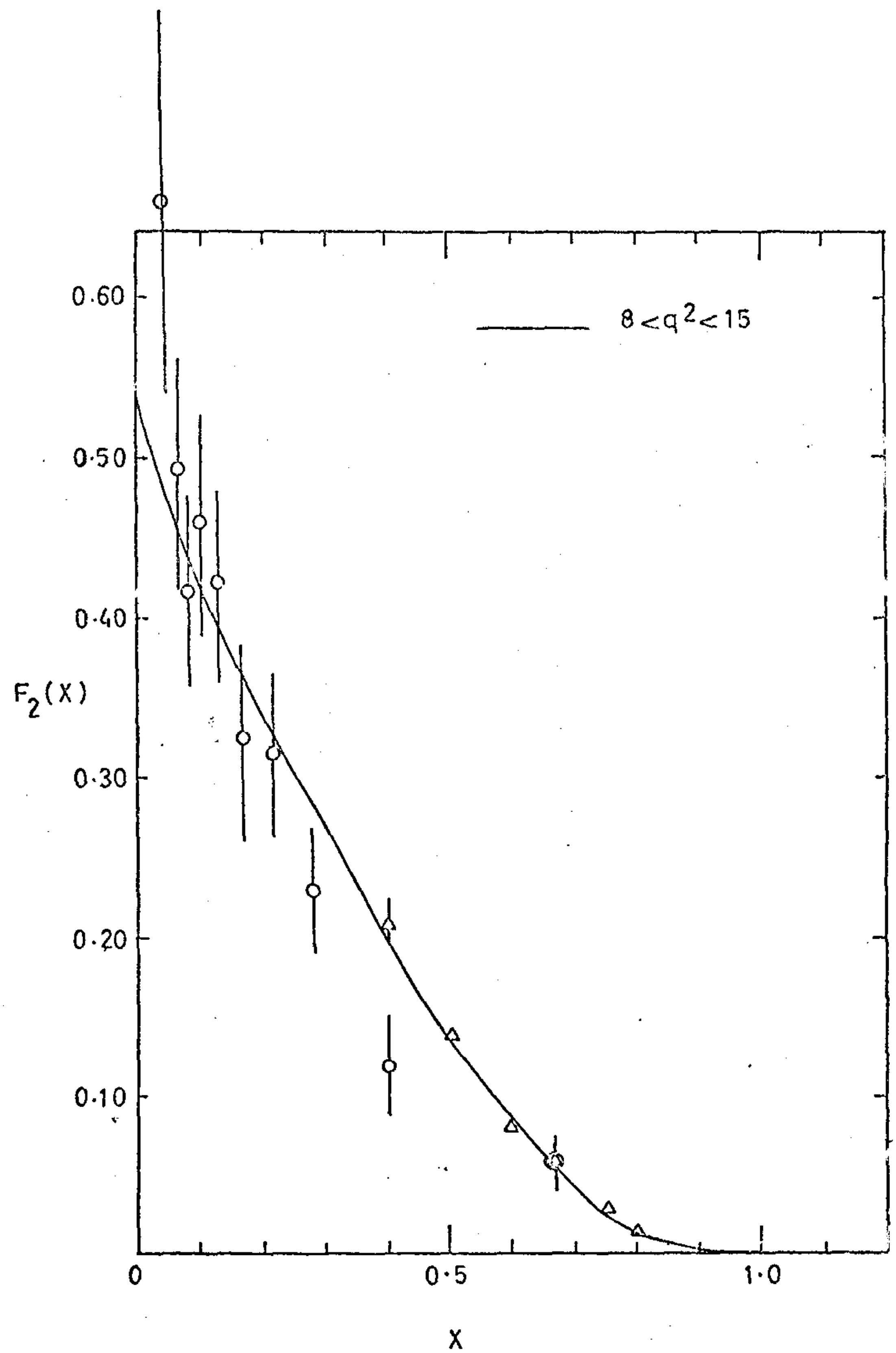

0.60
0.50
0.40
0.30
0.20
0.10
F2(X)
8<q2<15
0
0·5
1·0
X

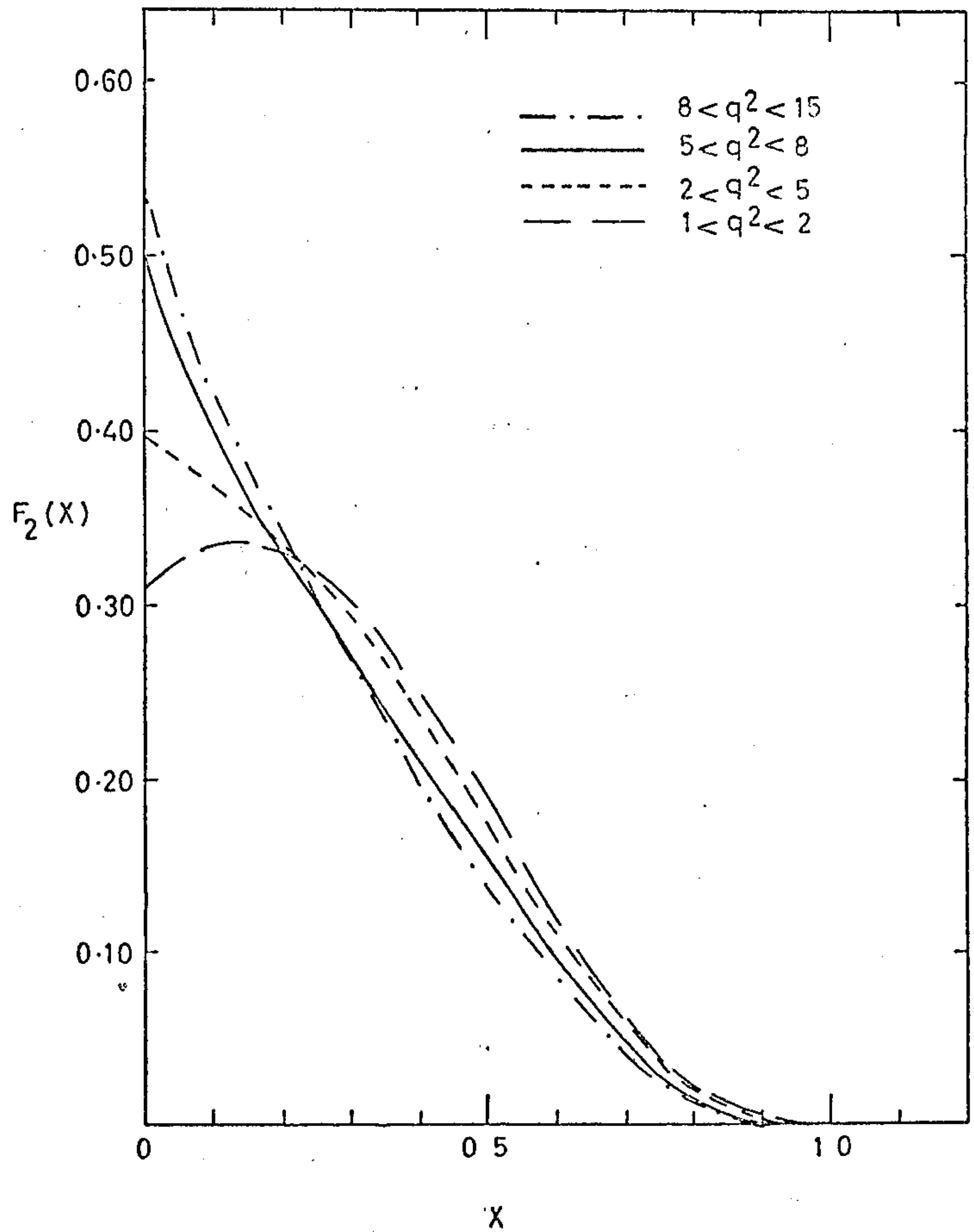

0·60
0·50
0·40
0·30
0·20
0·10
$F_2(X)$
0
0 5
1 0
X
$8 < q^2 < 15$
$5 < q^2 < 8$
$2 < q^2 < 5$
$1 < q^2 < 2$

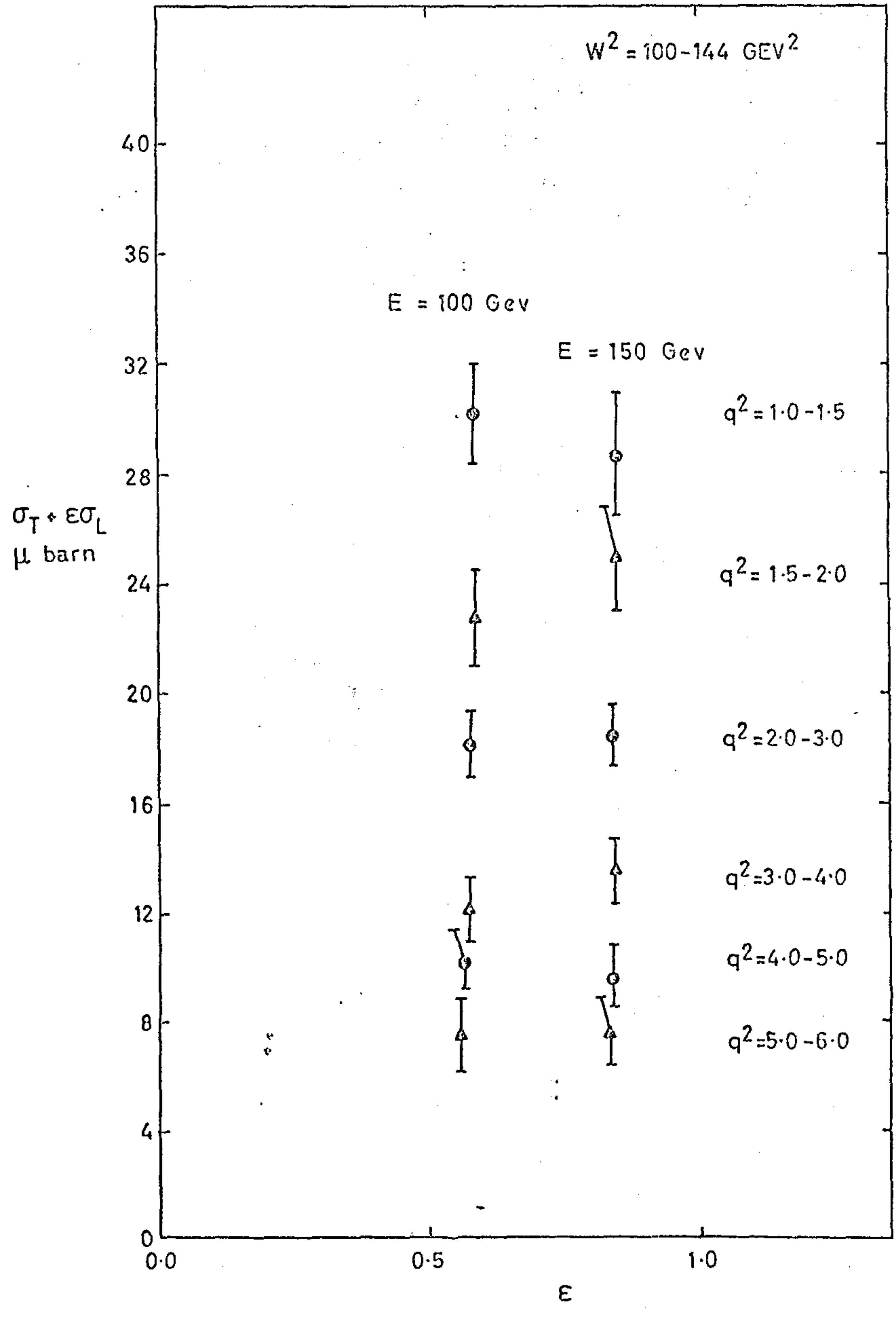

W² = 100-144 GEV²
E = 100 Gev
E = 150 Gev
q² = 1·0 - 1·5
q² = 1·5 - 2·0
q² = 2·0 - 3·0
q² = 3·0 - 4·0
q² = 4·0 - 5·0
q² = 5·0 - 6·0
σT + εσL
μ barn
40
36
32
28
24
20
16
12
8
4
0
0·0
0·5
1·0
ε